Report No. UCB/SEMM-2014/02	Structural Engineering Mechanics and Materials
	Collapse of a Concrete Wall Building in the 2010 Chile Earthquake By Ahmet Can Tanyeri, and Jack P. Moehle
March 2014	Department of Civil and Environmental Engineering University of California, Berkeley

COLLAPSE OF A CONCRETE WALL BUILDING IN THE 2010 CHILE EARTHQUAKE

Ahmet Can Tanyeri and Jack P. Moehle

ABSTRACT

On 27 February 2010, a M_w 8.8 earthquake occurred off the coast of central south Chile. The 15-story Alto Rio building in Concepción sustained failures near the base, overturned, and came to rest on its side. The collapse of the Alto Rio building was significant because it was designed using the Chilean Building Code NCh433.Of96 requires the use of ACI 318-95 for design of reinforced concrete structural elements intended to resist design seismic forces. It is the first modern shear wall building to collapse by overturning during an earthquake.

This study aims to demonstrate a practical approach to assessing the collapse of a complex building subjected to earthquake shaking, using the building plans and a post-earthquake reconnaissance report, reasons of collapse are investigated with linear elastic, nonlinear static, and nonlinear dynamic analyses. The results of analyses and failures identify details of the failure mechanism and suggest areas for which design and detailing practices could be improved.

INTRODUCTION

On 27 February 2010, at 03:34 local time (06:34 UTC), a M_w 8.8 earthquake occurred off the coast of central south Chile. The earthquake affected an area with population exceeding twelve million people, including five of the largest cities of Chile. The number of confirmed deaths stood at 525, with 25 people missing (Ministry of Interior, 2011). The earthquake caused damage to buildings, highways, railroads, ports, and airports, including 81,000

destroyed residential structures (EERI, 2010). At least 50 multi-story reinforced concrete buildings were severely damaged and four collapsed partially or totally. Among these, the 15-story Alto Rio building in Concepción sustained failures near the base, overturned, and came to rest on its side, with eight fatalities (Figure 1). Details of the collapse, and analyses to understand it, are the subject of this paper.

RESEARCH SIGNIFICANCE

The failure of the Alto Rio building is significant for many reasons. It is the first shear wall building of its type to collapse by overturning during an earthquake. The failures suggest areas for which design and detailing practices could be improved. The analyses demonstrate a practical approach to assessing the collapse of a complex building subjected to earthquake shaking. The capabilities and shortcomings of the analyses to identify details of the failure mechanism are themselves important outcomes of the study.

GROUND MOTION RECORDS IN CONCEPTION

The 2010 Chile earthquake had a moment magnitude of 8.8, which was the sixth largest earthquake ever to be recorded by a seismograph. According to the Seismological Service of the University of Chile, Concepción experienced strong ground shaking at Modified Mercalli Index IX (violent). Concepción was located 105 km (65.2 miles) from the estimated epicenter (35.909°S, 72.733°W; USGS 2010). Ground motions were recorded at Colegio Inmaculada Concepción (36.8281°S, 73.0483°W) (RENADIC 2010) in Concepción approximately 1.2 km (0.75 miles) from the Alto Rio site. Ramirez and Vivallos (2009) presents a study dividing Concepción into six different zones based on dominant periods and type of soil. This study shows that the Alto Rio building and Colegio Inmaculada Concepción sites are located in the same zone formed by alluvial deposits of the Bio-Bio River. The proximity of the sites

and the similar site characteristics suggest that the motions at the two sites may be reasonably similar, although deviations due to different wave paths are to be expected. The records (Figure 2) show that shaking lasted more than 120 seconds, with peak ground accelerations of 0.402g and 0.397g in east-west (EW) and north-south (NS) directions, respectively. The east-west direction of the record corresponds to the transverse (short) axis of the building.

Figure 3 compares 5-percent-damped elastic response spectra computed using the records and design-level response spectra based on the Chilean code NCh433.Of96 for seismic zone 3 and building category C. Design response spectra are shown for two soil types. Soil Type II corresponds to stiff soil whereas Soil Type III corresponds to medium stiff soil. Soil Type II represents a dense gravel or clay with shear wave velocity larger than 400 m/s in the upper 10 m (32.2 ft), and Soil Type III is unsaturated gravel or clay with shear wave velocity less than 400 m/s (NCh433.Of96, 1996). Spectral accelerations for the earthquake are at or above the Type II soil design spectrum for almost all periods. The EW direction motions are particularly energetic in the approximate period range 1.5s to 2.5s.

CHILEAN DESIGN PRACTICE FOR RC BUILDIGNS

A long history of frequent strong earthquakes in Chile has resulted in the nearly universal use of bearing walls for mid-rise concrete residential construction. In a typical layout (Figure 4), corridor walls are flanked by transverse walls forming room partitions. A typical ratio of wall area to floor plan area is around three percent in each direction (Wallace and Moehle, 1992). This ratio has remained relatively constant over the years, but building heights have increased with time, leading on average to higher axial stresses at the building base. Wall thicknesses have also decreased over time; at the time of the earthquake, it was not unusual to find 15 to 20 cm (5.9 to 7.9 in) thick walls supporting 15 to 20-story tall buildings.

The Chilean Building Code NCh433.Of96 requires the use of ACI 318-95 for design of

reinforced concrete structural elements intended to resist design seismic forces. However, based on satisfactory behavior of walls in past earthquakes, wall designs were not required to satisfy the ACI 318 requirements for confined boundary elements. The Chilean Reinforced Concrete Code was modified in 2008 to require use of confined boundary elements. Several Chilean engineers have indicated, however, that this requirement was not always followed in design, and confinement, where specified, was not always implemented in construction.

ALTO RIO BUILDING

The Alto Rio building was a 15-story reinforced concrete building with two additional subterranean levels. It had a nearly rectangular plan (Figure 4 and Figure 5) with the transverse (short) direction oriented on 60 degrees azimuth, which corresponds to the EW direction of the ground motion in Figure 2. The building plan dimensions were 40 m (131 ft) in the longitudinal direction and 12 m (39 ft) in the transverse direction. The building had stepped elevation at the roof, such that it was 12 stories tall at the north end and 15 stories tall at the south end, with maximum height of 38 m (125 ft). First-story height was 3.06 m (10 ft) and all other stories including subterranean levels were 2.52 m (8.3 ft) tall.

At the time of design in 2006, the applicable building code was NCh433.Of96, which referred to ACI 318-95. The building was designed using analysis and design procedures similar to those used in the US, including linear elastic response spectrum analysis using the computer program ETABS (CSI). Building construction was completed in 2009.

The seismic-force-resisting system comprised a pair of longitudinal corridor walls flanked by transverse walls, and interconnected by 150-mm (5-in.) thick floor slabs. Along axes 8, 13, and 20, the first-story transverse walls were continuous along the entire building width. Above the first story, a stack of 1.2 m (4 ft) wide corridor openings divided these into two separate walls coupled by floor slabs (Figure 6 and 8). The easternmost edge of these

walls, as well as the shorter walls along axes 11, 17, and 24, had another discontinuity at the second level where the first story was set back 40 cm (1.31 ft) from the upper stories on the east side of the building (Figure 7). Above the setback, the walls had a return at the exterior face of the building, exacerbating the vertical discontinuity in the framing system.

Walls were 20-cm (7.9 in) thick, except some underground walls were 25-cm (9.8 in) thick. Wall distributed reinforcement comprised either ϕ8* or ϕ10 with 15 or 20-cm (5.9 or 7.9 in) spacing. Larger diameter longitudinal bars (ϕ16 to ϕ25) were positioned at the wall boundaries. The structural drawings show wall transverse reinforcement detailed with 135-degree hooks anchored around wall boundary reinforcement with typical longitudinal (vertical) spacing of 20 cm (7.9 in). A field survey after collapse showed that transverse reinforcement was constructed with 90-degree hooks (IDIEM 2010). Wall longitudinal reinforcement was lap-spliced according to conventional practices, without special confining transverse reinforcement along the lap splices. For ϕ22 mm and ϕ25 bars, lap splice lengths of 125 cm (49 in) ($57d_b$) and 140 cm (55 in) ($56d_b$) are provided in design. The length required by ACI 318-11 equation 12-1 for a Class B lap splice (all the bars spliced at the same level) developing specified yield stress is $43d_b$. According to ACI 318-11 21.9.2.3, regions of special structural walls that are expected to yield are required to have development lengths of longitudinal reinforcement at least 1.25 times the values calculated for f_y in tension, or a lap splice length of $54d_b$. Therefore, lap splice lengths meet requirements of ACI 318. In US practice, however, a special structural wall might be expected to have more and better detailed transverse reinforcement than is typical in Chilean practice. Given the transverse reinforcement detailing in Alto Rio, it is reasonable to suspect the lap splices as a potential initiator of failure.

All reinforcement was specified S420 steel [minimum yield strength of 420MPa (60 ksi) and ultimate strength of 630MPa (90 ksi)]. Consistent with the specification,

reinforcement samples taken from the collapsed building had mean yield and ultimate stresses of 484 MPa (70 ksi) and 727 MPa (105 ksi), respectively (IDIEM, 2010). From the base to the top of the second story, specified concrete compressive strength was 25 MPa (3600 psi); for the rest of the building specified compressive strength was 20 MPa (2900 psi). Thirty-three concrete cores taken from the structural walls after the earthquake showed mean compressive strength of 43 MPA (6200 psi), with somewhat lower strength in lower stories than upper stories. This result contrasts with the strength specification in that higher strengths were specified for the lower stories than upper stories.

The building was founded on alluvial deposits. Soil investigations reported by IDIEM (2010) indicate the building site had static strength parameters consistent with aspects of both Soil Type II and Type III (Table 1, Figure 9). Soil Type II corresponds to stiff soil whereas Soil Type III corresponds to medium stiff soil. Soil Type II represents a dense gravel or clay with shear wave velocity larger than 400 m/s in the upper 10 m (32 ft), and Soil Type III is unsaturated gravel or clay with shear wave velocity less than 400 m/s (NCh433.Of96, 1996). In order to be classified as Soil Type II, soil of that characteristic should have a minimum thickness of 20 m (65 ft); Soil Type III requires minimum thickness of 10 m (33 ft). Soil investigations reported by IDIEM (2010) indicate existence of both Soil Type II & III. However, all layers have shear wave velocities below 300 m/s, suggesting the soil should be classified as Type III.

The cross-sectional wall to floor area ratio was approximately 3% in the longitudinal direction and 4% in the transverse direction, resulting a total cross-sectional wall to floor area of 7%. Calculated wall axial load ratios ranged from 0.05 to 0.07 $P/f_c'A_g$, where P considers expected loads ($1.0D + 0.25L$), f_c' is the specified concrete compressive strength, and A_g is the gross cross-sectional area of the wall.

COLLAPSE

During the earthquake, the Alto Rio building overturned from the base level and came to rest on its east side (Figure 1). Examination of the building in its final resting place indicated that the main failure occurred in or near the first story, and that the building rotated approximately about the central corridor as it fell to the east. According to this mechanism, the west side of the building failed in tension whereas the east side failed in compression, with portions of the east side being thrust into the subterranean levels. A small amount of longitudinal movement was apparent where the building fractured at the base, but this appears to have occurred as the building collapsed, not beforehand (IDIEM, 2010). The building was also fractured at the ninth level, probably due to impact with the ground and walls of the adjacent parking structure, snapping the building in two as it hit the ground. Inspection of the foundation and soil did not identify significant damage.

Figures 10 and 11 show damage maps identifying the principal fractures near the base of the building along axes 5, 8, 11, and 13, including:

- Walls along axes 8 and 13 show apparent compression failures on the east side near the first level. Detailed surveys showed both concrete crushing and longitudinal reinforcement buckling. Wall piers along axes 11, 17, and 24 suffered similar failures at the setback level (between first and second floor).
- Large horizontal cracks along axes 5 and 8 indicate that the wall on the west side near the first level sustained significant tension, consistent with actions expected as the building overturned toward the east. Photographs of the failure interface on the west side showed both fractured bars and failed lap splices. Similar damage was absent on the east side, although such damage would have been obscured by crushing failures on that side.

- The solid wall panels in the first story, just below the stack of corridor openings, sustained major damage (axes 5, 8, and 13). Damage in these panels may be due to large shear forces that result from opposing tension and compression forces in the wall boundaries adjacent to the corridor. Such "solid wall panels" have been damaged in past earthquakes (Naeim et al. (1990)).

Based on the damage inspection alone, the authors are unable to identify which of the major damage types (concrete crushing, reinforcement tension failure, or wall panel failure) occurred first or was the major trigger for the collapse. To gain further insight into the collapse, analytical studies were conducted, as described in the following sections.

LINEAR ELASTIC RESPONSE SPECTRUM ANALYSIS

A linear elastic model of the Alto Rio building was prepared using the computer program ETABS (CSI). Shear walls were modeled using shell elements. Effective flexural stiffness was defined as $E_c I_{eff} = 0.5 E_c I_g$ in accordance with ASCE 41-06, in which E_c = Young's modulus of concrete (assumed 30,820 MPa (4,470 ksi) for both C20 and C25 concretes), I_{eff} = effective second moment of inertia of the section, and I_g is the second moment of inertia of the gross section. Values of E_c are from ACI 318-11 using concrete strength values from the concrete core tests conducted after the earthquake (IDIEM, 2010). The same reduction factor (0.5) applies to shear and axial stiffness as well. Effective seismic mass on each floor was calculated as $m_s = m_d + 0.25 m_l$, in which m_d is mass of self-weight and dead loads, and m_l is mass corresponding to the design live load (2.0 kPa (0.29 psi) typically). Slabs had infinite in-plane stiffness with no out-of-plane flexural stiffness. The model includes flexibility of walls and columns extending below grade level, but lateral translational degrees of freedom are fixed at grade and subterranean levels, and vertical translational degrees of freedom are fixed at the lowest subterranean level.

Table 2 lists calculated periods and primary directions. The calculated fundamental periods in the transverse and longitudinal directions correspond to $N/19$ and $N/21$, respectively, which are typical of values for Chilean shear wall buildings (Wallace and Moehle, 1989).

Response spectrum analysis was done using 2.5%-damped response spectra for the recorded Concepción ground motions, with results combined using the complete quadratic combination method (Der Kiureghian and Nakamura, 1993). The effective damping value was selected based on recommendations of PEER/ATC-72-1 (2010). Calculated roof displacements were $0.0070h$ and $0.0046h$ in the transverse and longitudinal directions, respectively, where h = height from grade level to top of the roof at the 15th level. Maximum inter-story drifts were $0.0090h_x$ and $0.0069h_x$ in the transverse and longitudinal directions, where h_x = story height. As a point of reference, maximum permitted story drift ratio for this building type is $0.02h_x$ in ASCE 7-10. The linear model showed stress concentrations in the walls around the setback at level 2 and in the solid panels beneath the stacks of openings. Numerical values of stress were sensitive to mesh size, and are not reported here.

NONLINEAR STATIC ANALYSIS

To gain further understanding of the inelastic behavior of the building, a static lateral force analysis was conducted on an analytical model representing the inelastic material properties of a portion of the building in the transverse direction. Only the walls along axes 8 and 13 were modeled, as these were deemed representative of the main portion of the seismic-force-resisting system of the building. Contributions of the walls along axes 11 and 17 are ignored in the analysis, as these are not likely to contribute significantly to overall lateral resistance. Figures 4 and 5 indicate the portion of the building included in the model.

An important first step in developing an inelastic model is to identify the likely modes

of inelastic response. Inelastic flexural response of the walls is an obvious consideration. Typical of Chilean design practice, the Alto Rio building features a pair of longitudinal corridor walls flanked by transverse walls, resulting in a series of T and L-shaped wall cross sections (Figures 4 and 5). Given the slender aspect ratio of the walls, the flanges can be assumed to be fully effective as either a compression or tension element, depending on the loading direction. Such walls are relatively strong but brittle for loading that puts the flange in tension and the stem in compression, and relatively weak but ductile for loading in the opposite direction. Figure 12 plots calculated moment-curvature relationships of a T-shaped shear wall along axis 13 for expected axial loads (1.0D + 0.25L), demonstrating the asymmetry in load-deformation response. Where two such walls are placed with their flanges back-to-back to create a corridor, the result is one T-wall that is strong and brittle while the other is weak and ductile. Under lateral load, the strong wall attracts greater force and degrades earlier than the other wall. These interactions can be monitored using a structural analysis model of the building that incorporates the inelastic flexural response characteristics.

Another potential source of inelastic response results from the high shear stress that develops in the solid wall panel directly beneath a stack of openings. This stress is the result of opposing flexural tension and flexural compression forces in the boundaries of the walls on opposite sides of the opening (Figure 13). Studies (for example, Naeim et al., 1990) show that the majority of this force is resolved by panel zone shear stresses that occur within a short distance below the bottom of the stack of openings. The effect is analogous to the shear stress that develops in beam-column joints of moment-resisting frames. Studies of typical Chilean buildings show that this stress may reach the stress capacity of the panel (ATC 94, 2013). Therefore, a nonlinear model of the building should also represent this effect.

Nonlinear static analysis was carried out using the computer program Perform3D (CSI). Structural walls were modeled using 4-noded “Shear Wall Elements” (CSI) with fiber

cross sections. In this implementation, all interconnected planar wall segments at any level are assumed to remain plane when deformed. In the first and second floor, where inelastic actions were expected to concentrate, shear wall elements were meshed so that each element had a height of twice the wall web thickness. This value was established from post-earthquake observations of the typical height of spalled and crushed regions. For the rest of the building, larger-sized elements were used.

Materials for the fiber elements were modeled based on the mean test results from coupons taken after the earthquake. The concrete stress-strain relation for compression was a trilinear relation with a descending portion (Figure 14). Concrete was assumed to be unconfined because of the wide spacing and 90-degree hooks on the transverse reinforcement. It was assumed that concrete has no tension resistance.

The reinforcing steel stress-strain relation for the fiber elements was modeled using the relation shown in Figure 15. The ultimate strain in tension was limited to 0.05 in consideration of low-cyclic fatigue (PEER/ATC-72-1). Behavior in compression was varied according to the ratio s/d_b (s = spacing of transverse reinforcement and d_b = diameter of longitudinal bar) in consideration of longitudinal bar buckling (Monti and Nuti, 1992). It was assumed that bar buckling could not trigger spalling, but instead buckling could occur only following spalling of cover concrete at assumed compressive strain of 0.005. Some ongoing research suggests that reinforcement buckling can initiate spalling under some circumstances, but this possibility was not modeled.

An inelastic shear material was used for the walls, with nominal shear strength of $1.5V_n$, in which V_n is the nominal shear strength defined in ACI 318-11, that is, $V_n = \left(0.17\sqrt{f_c'} + \rho_t f_{yt}\right)A_{cv}$ (MPa) $\left[\left(2\sqrt{f_c'} + \rho_t f_{yt}\right)A_{cv}\text{ (psi)}\right]$, in which ρ_t = transverse reinforcement ratio, f_{yt} = yield stress of transverse reinforcement, and A_{cv} = web area of wall. The solid wall panels beneath the stack of openings were modeled in two different ways. In

one model, the regions were modeled with an elastic shear material having effective shear stiffness defined as $0.4E_cA_{cv}/20$ (PEER/ATC-72-1), in which $0.4E_c$ approximates the shear modulus G_c and the divisor 20 represents stiffness reduction associated with concrete cracking. In a second model, the solid wall panels were modeled using a trilinear shear material having initial stiffness $0.4E_cA_{cv}$, with the first break point at shear equal to $0.33\sqrt{f_c'}A_{cv}$ (MPa) [$4\sqrt{f_c'}A_{cv}$ (psi)], followed by a strain-hardening branch to a point defined by the intersection of a shear force of $1.5V_n$ and a secant from the origin at a slope of $2.5\rho_t nG_c$, in which ρ_t is the ratio of the area of horizontal reinforcement to the area of concrete, $n = E_s/E_c$ is defined as the modular ratio, and G_c is the shear modulus of concrete (= $0.4E_c$). The shear model degrades after reaching shear force $1.5V_n$. This model was based on the recommendation in Sozen et al. (1992) and was found to correlate well with the test results of similar wall panels reported in Vecchio and Collins (1986). The force transfer between the panel zone and the adjacent walls is achieved through the assumption of the perfect bond of the boundary element reinforcement from the walls into the solid segment.

The analytical model was subjected first to gravity loads and then to progressively increasing lateral forces. Gravity loads were estimated based on tributary areas for the various walls, considering $1.0D + 0.25L$ (D = dead load and L = specified live load). For lateral analysis, an inverted triangular force pattern was applied at the center of mass of each floor of the modeled part of the building. Due to the tendency for some torsional response for this loading, rotations about a vertical axis were artificially prevented.

Figure 16 shows calculated relations between base shear and roof displacement for east and west loading directions of the model with nonlinear shear stress-strain relationships assigned to the solid panel beneath the corridor openings and the rest of the model. For loading the model to the east, the direction in which collapse occurred, the first significant event is crushing of the wall boundary at the east edge of the east wall along axis 13 at

around 0.72% roof drift ratio, followed by similar crushing of the east part of wall 8 at around 1% roof drift ratio. The crushing occurs at the transition between levels 1 and 2, apparently because of the wall vertical discontinuities at that level (the setback between stories 1 and 2 and beginning of the stacked openings along the corridor). Compression failure of the east side of the walls along axes 13 and 8 resulted in numerical instability of the model. It is noteworthy that at the roof drift corresponding to the crushing of W8-E, the model indicates boundary reinforcement tensile strain of 5 to 14 times the yield strain. Thus, it plausible that the lap splices may have sustained some yielding and strength degradation before this point.

For lateral load to the west, the first significant events are failure of the solid wall panels below the stack of openings between coupled walls along axes 8 and 13 at around 0.9% roof drift ratio. "Failure" is arbitrarily defined as onset of strength degradation after reaching shear strength $1.5V_n$. This is followed by fracture of the longitudinal reinforcement at the east side of the east walls along Axis 13 at 1.6% roof drift ratio. (The drift estimates corresponding to fracture are likely to be low because of the small element size, which can result in strain concentration in the reinforcing steel model. Sensitivity studies have been done in order to investigate the effect of mesh size on the response. There was no significant relationship observed between element sizes and drift ratios corresponding to the fracture of reinforcing steel.) It is noteworthy that crushing failure is not calculated to occur for loading in this direction, at least not within the drift range of interest. Apparently, the absence of the setback and the short returns on the walls result in sufficient compression area to avoid crushing failure for loading to the west.

The calculated maximum shear force resisted by the walls along axes 8 and 13 is 4400 kN (990 kips) for loading to the east and around 5000 kN (1125 kips) for loading to the west. Nominal shear strength V_n calculated according to ACI 318-11 is 9300 kN (2090 kips). Shear forces could increase for alternative lateral loading patterns, especially where building

response extends well past the effectively linear range of response (Rejec et al., 2011). Crushing of the walls, however, effectively preempts development of ductile flexural response, thereby reducing the likely shear force amplification. Therefore, it seems highly unlikely that the shear demands reached the shear capacity, or that wall shear failure was a primary initiator of the collapse. The single exception is the solid wall panel immediately below the stack of openings.

Figure 17 shows the calculated relations between roof drift ratio and (a) average shear stress in the solid wall panel below the stack of openings (solid line) and (b) average shear stress across the entire wall length (dashed line). The results are for the model loaded in the collapse direction, with the solid wall panel below the stack of openings modeled as linearly-elastic. The average stress in the solid wall panel below the stack of openings is approximately three times the average stress acting across the entire wall section. This result is consistent with the results reported by Naeim et al. (1990).

Figure 18 shows the calculated relation between shear stress and shear strain in the solid wall panel below the stack of openings for the model in which the solid wall panel is modeled using an inelastic shear material, as described previously. Lateral loading is toward the east. Inelastic response of the region is apparent. More significant inelastic response of the solid wall panel is obtained for loading toward the west (not shown). Overall, the calculated results are consistent with reported damage, which shows cracking or destruction of the solid wall panel below the stack of openings (see Figures 10 & 11).

It is noteworthy that wall crushing damage and solid wall panel shear damage are estimated to occur for roof drift ratio in the range 0.007 to 0.010 for loading toward the east, with similar effects at higher drifts for loading toward the west (Figure 16, 18). As reported previously in this paper, linear response spectrum analysis indicates that the roof drift ratio demand was approximately 0.007 in the transverse direction, similar to the drift at onset of

critical damage. To better understand dynamic response, a series of simplified nonlinear dynamic models were studied.

DYNAMIC SDOF ANALYSIS

A single-degree-of-freedom (SDOF) model was established to represent the effective first translational mode response of the Alto Rio building in the transverse direction. The SDOF model was implemented in Perform3D with a nonlinear rotational spring at the base, a massless rigid bar, and a mass at the top. Mass and height of the rigid bar are effective modal mass, M_1^*, and effective modal height, h_1^*, of the fundamental vibration mode (Chopra 2011), defined by:

$$M_1^* = \frac{\sum_{r=1}^{j}(m_r\varphi_r)^2}{\sum_{r=1}^{j} m_r\varphi_r^2} \quad (1)$$

$$h_1^* = \frac{\sum_{r=1}^{j} m_r\varphi_r h_r}{\sum_{r=1}^{j} m_r\varphi_r} \quad (2)$$

in which φ_r is the r^{th} story value of the first-mode shape, m_r is the mass matrix value of the r^{th} story, h_r is the height of r^{th} story level from the base level, and j is the number of stories.

The moment-rotation relationship of the rotational spring is based on the base moment versus roof drift relationship resulting from the nonlinear static analysis of the structure (Figure 19). Because the nonlinear static analysis results are only for a representative part of the structure, they should be adjusted to represent the response characteristics of the entire building. Recognizing the approximate nature of the scaling process, we simply scaled the moment values of the relationship by the ratio of seismic mass of the whole building to the seismic mass of the portion of the structure included in the nonlinear static analysis. The initial slope of the moment-rotation response was selected to match the fundamental vibration period calculated using ETABS, described previously. Other parameters of the simplified trilinear moment-rotation relation were adjusted to approximate the relation obtained with the

scaled nonlinear static analysis, as shown in Figure 19. Hysteresis rules governing unloading and reloading stiffness and energy dissipation per cycle were implemented to approximate the approach presented by Saiidi and Sozen (1981). The SDOF model was excited with the east-west direction of the ground motions recorded at Colegio Inmaculada Concepción site.

Calculated moment-drift relations and displacement response histories of the SDOF model subjected to the Concepción motion are plotted in Figures 20 and 21. It is worth noting that after a deformation cycle as large as 1.3% roof drift ratio in the west direction, the SDOF model collapses to the east (collapse) direction at around 22 seconds of the excitation. The final result of the dynamic SDOF analysis is consistent with the observed damage and collapse of the building.

To assess the influences of fundamental period and base moment capacity of the SDOF model on the calculated response, a sensitivity study was conducted. Varying values of fundamental periods from 0.4 seconds to 1.2 seconds (increments of 0.1 seconds), and values of base moment capacity from 0.5 to 1.5 (increments of 0.1) times the calculated moment capacity were used in the analysis. All combinations resulted in collapse of SDOF model in the east (collapse) direction. This result suggests that the collapse was insensitive to strength and stiffness, and instead was driven by the brittle behavior of the structure.

The nonlinear static and dynamic SDOF analysis results demonstrate that the Alto Rio building was susceptible to collapse to the east direction. The main factors contributing to the failure include: the configuration of T and L-shaped wall cross sections, vertical discontinuities at the east side of the building, and high shear stresses in the solid wall panels below the stack of openings. The structural drawings and reconnaissance data suggest that the absence of confined boundary elements and the occurrence of lap splices of longitudinal bars without sufficient transverse reinforcement could be other factors that contributed to the collapse. The specific analyses reported in this paper indicate one plausible failure sequence,

that is, initiation of shear damage in the solid wall panel immediately below the stack of openings, crushing and buckling failure of the walls at the discontinuity between the first and second stories on the east side of the building, and subsequent failure of the tension chord on the west side of the building as it collapsed toward the east. Other failure sequences are also plausible, depending on details of the ground motion and structural model, but these were not indicated by the present study. Observed damage after the earthquake (IDIEM, 2010) is consistent with the findings of the analysis results.

SUMMARY AND CONCLUSIONS

The M_w 8.8 2010 Maule Chile earthquake affected over twelve million people in central south Chile, severely damaging more than 50 multi-story reinforced concrete buildings and causing partial or total collapse of four other such buildings. Among these, the 15-story residential Alto Rio building stands out as the first modern shear wall building to collapse by overturning during an earthquake. The recorded ground motions approximately 1.2 km (0.75 miles) away from Alto Rio show that shaking lasted more than 120 seconds with peak ground accelerations of 0.402g and 0.397g in east-west and north-south directions, respectively. Using the building plans and a post-earthquake reconnaissance report, reasons of collapse are investigated with linear elastic, nonlinear static, and nonlinear dynamic analyses.

A linear elastic model of the whole Alto Rio building was prepared using effective (cracked) section properties of the structural elements. The fundamental periods in transverse and longitudinal directions were typical of values for Chilean wall buildings, with values of $N/18$ and $N/20$, respectively, where N = number of stories. Calculated wall axial load ratios ranged from 0.05 to 0.07 $P/f_c'A_g$, where P considers expected loads (1.0D + 0.25L).

A nonlinear static analysis was conducted on an analytical model representing inelastic material properties of walls along axes 8 and 13 in the building transverse direction; this

portion was deemed representative of the seismic-force-resisting system of the building. The model was loaded with an inverted triangular lateral force pattern. For loading to the east (collapse) direction, critical lateral strength degradation occurred due to crushing of the wall boundary at the east edge of the east wall along axis 13 at around 0.7% roof drift ratio, followed by similar crushing of the east part of wall along axis 8 around 1.0% roof drift ratio. The crushing zone occurred adjacent to a vertical discontinuity in the wall cross section. Solid wall panels beneath the stack of openings were calculated to undergo cracking and inelastic response, without failure, for loading in this direction. For lateral load toward the west, those same solid wall panels sustained shear failures, as indicated by initiation of shear strength degradation, at approximately 0.9% roof drift ratio. This was followed by fracture of the longitudinal reinforcement at the east side of the east walls along Axis 13 at 1.6% roof drift ratio. Apart from the isolated shear failure of the solid panel beneath the stack of openings, analyses indicate that shear failure was not an initiator of building failure.

Dynamic analysis of a single-degree-of-freedom (SDOF) model was established to represent the effective first translational mode response of the Alto Rio building in the transverse direction. The SDOF model was excited by the ground motions recorded in Concepción, 1.2 km (0.75 miles) away from Alto Rio. Studies using this model indicate that building collapse would occur toward the east, as observed following the earthquake, and that this result was relatively insensitive to the properties of the SDOF model.

The results of this study suggest that the Alto Rio building was susceptible to collapse to the east direction due to the following main factors:

1. The configuration of T and L-shaped wall cross sections resulted in low deformation capacity for loading that placed the flange in tension and the stem in compression.

2. Vertical discontinuities at the east side of the building created stress concentration at the top of the first story, with corresponding damage concentration.
3. The solid wall panels below the stack of corridor openings were susceptible to high shear demands and shear damage.

Other potential contributing factors include the absence of confined boundary elements and the presence of lap-spliced longitudinal reinforcement without confining transverse reinforcement.

ACKNOWLEDGMENTS

This work was supported in part by the Earthquake Engineering Research Centers Program of the National Science Foundation under Award No. 0618804. Computers and Structures, Inc. generously donated the software PERFORM 3D and ETABS. The authors thank John Wallace and Zeynep Tuna for their collaboration and comments on this study. Any opinions, findings, and conclusion or recommendations expressed in this work are those of the writers and do not necessarily reflect those of the organizations or individuals noted here.

REFERENCES

1. ACI 318-95 (1995), "Building Code Requirements for Structural Concrete (ACI 318-95) and Commentary," American Concrete Institute, Farmington Hills, Michigan.
2. ACI 318-11 (2011), "Building Code Requirements for Structural Concrete (ACI 318-11) and Commentary," American Concrete Institute, Farmington Hills, Michigan.
3. American Society of Civil Engineers (2006), "Seismic Rehabilitation of Existing Buildings", ASCE Standard ASCE/SEI 41-06.
4. American Society of Civil Engineers (2010). "ASCE/SEI 7-10: Minimum Design Loads for Buildings and Other Structures," Reston, VA, 650 pp.

5. ATC 94 (2013). “Recommendations for Seismic Design of Reinforced Concrete Wall Buildings based on Studies of the 2010 Chile Earthquake,” NIST GCR 13-917-25, National Institute of Standards and Technology.
6. Chopra, A. K. (2011). “Dynamics of Structures Theory and Applications to Earthquake Engineering Fourth Edition”, Prentice Hall, Upper Saddle River, NJ.
7. Computers and Structures, Incorporated (CSI), “Perform 3D, Nonlinear Analysis and Performance Assessment for 3D Structures”, Berkeley, CA
8. Computers and Structures, Incorporated (CSI), “ETABS Nonlinear, Extended 3D Analysis of Building Structures, Computers and Structures”, Berkeley, CA
9. Der Kiureghian, A., and Y. Nakamura (1993). CQC modal combination rule for high-frequency modes. Earthquake Engineering and Structural Dynamics, 22(11), 943-956
10. Earthquake Engineering Research Institute, (2010). "EERI Special Earthquake Report-June 2010: The Mw 8.8 Chile Earthquake of February 27, 2010," Oakland, CA.
11. IDIEM (2010). “Peritaje Estructural Edificio Alto Río, Ciudad de Concepción, Informe Final, Descripción de Caida y Factores Asociados al Colapso, Revisión 1,” Informe No 644.424-00, Centro de Investigación, Desarrllo e Innovación de Estructuras y Materiales (IDIEM), University of Chile.
12. Monti, G., and Nuti, C. (1992), “Nonlinear Cyclic Behavior of Reinforcing Bars Including Buckling,” Journal of Structural Engineering, American Society of Civil Engineers, 118(12), 3268-3284.
13. Naeim F., B. Schindler, J.A. Martin, and S. Lynch (1990). “Hidden Zones of High Stress in Seismic Response of Structural Walls,” Proceedings, 1990 Structural Engineers Association of California Convention, pp. 402-422.

14. Official Chilean Code NCh 433.of.96. (1996). “Seismic Design of Buildings”, Instituto Nacional de Normalizacion, Santiago, Chile.
15. PEER/ATC-72-1 (2010), “Modeling and Acceptance Criteria for Seismic Design and Analysis of Tall Buildings,” Applied Technology Council, Redwood City, CA.
16. Ramirez, P., and Vivallos, J., 2009. Microzonificacion Sismica de la Ciudad de Concepción, Chile, in XII Congreso Geologico Chileno, Santiago, Chile.
17. Rejec, K., T. Isaković, and M. Fischinger (2011). “Seismic shear force magnification in RC cantilever structural walls designed according to Eurocode 8,” Bulletin of Earthquake Engineering, DOI 10.1007/s10518-011-9294-y, 20 pp.
18. Renadic (2010). “Red de Cobertura Nacional de Acelerografos”, Departamento de Ingenieria Civil, Facultad de Ciencias Fisicas y Matematicas, Universidad de Chile
19. Saiidi, M., and Sozen, M. A. (1981), “Simple Nonlinear Seismic Analysis of R/CStructures,” Journal of Structural Engineering, American Society of Civil Engineers, 107(ST5), 937-952.
20. Sozen, M.A., P. Monteiro, J.P. Moehle and H.T. Tang (1992). “Effects of Cracking and Age on Stiffness of Reinforced Concrete Walls Resisting In-Plane Shear,” Proceedings, Fourth Symposium on Current Issues Related to Nuclear Power Plant Structures, Equipment and Piping, Orlando, Florida, December 9-11, 1992.
21. U.S. Geological Survey (USGS), (2010). USGS Earthquake Hazards Program: Magnitde 8.8 – Offshore Bio-Bio, Chile, available at earthquake.usgs.gov/earthquakes/eqinthenews/2010/us2010tfan/
22. Vecchio, F.J, Collins, M.P., (1986). “The Modified Compression-Field Theory for Reinforced Concrete Elements Subjected to Shear”, ACI Journal, Proceedings V. 83 No. 2, March-April 1986, pp. 219-231.

23. Wallace, J.W., Moehle, J.P., (1989). “The 1985 Chile Earthquake: An Evaluation of Structural Requirements for Bearing Wall Buildings,” Report N° UCB/EERC-89-05.
24. Wallace, J.W., Moehle, J.P., (1993). “An Evaluation of Ductility and Detailing Requirements of Bearing Wall Buildings Using Structural Walls,” Journal of Structural Engineering, pp. 121(1).

TABLES AND FIGURES

List of Tables:

List of Figures:

Fig. 13 – (a) Region of high shear stress in solid wall panel below the stack of openings (b) Solid wall panel shear and tension/compression chords

Fig. 14 – Concrete stress-strain relation

Fig. 15 – Reinforcing steel stress-strain relation

Fig. 16 – Base Shear – Drift relationship of nonlinear static analysis

Fig. 17 – Shear stress – roof drift ratio relationship for solid wall panel below the stack of openings and for entire wall in story 1, using a linear model for the solid wall panel. Stress for the solid wall panel is the average value over the height of the story below the stack of openings

Fig. 18 – Shear stress – strain relationship of the solid wall panel below the stack of openings along axis 13 of the Alto Río building

Fig. 19 – Comparison of moment-rotation relations for the SDOF model and the scaled nonlinear static analysis

Fig. 20 – Moment–drift ratio response of the SDOF model under the Concepción ground motion

Fig. 21 – Roof drift ratio response history of the SDOF model subjected to the Concepción ground motion

Table 1 – Soil Properties of Alto Rio
(Note: 1 ft = 0.3048 m, 1 MPa = 145 psi)

Layer	Soil Characteristic	Test Result	Soil Type
1	Sandy Soil Layer	$(N_1)_{60} = 38$ / ft	III
2	Silty Soil Layer	Su = 0.12 MPa	II
3	Sandy Soil Layer	$(N_1)_{60} = 36$ / ft	III
4	Sandy Soil Layer	$(N_1)_{60} > 50$ / ft	II

Table 2 – Calculated vibration periods

Mode	Period (s)	Direction
1	0.81	Transverse
2	0.71	Longitudinal
3	0.58	Torsional
4	0.19	Longitudinal
5	0.17	Transverse
6	0.14	Torsional

Fig. 1 - Alto Rio building after the earthquake (from http://skyscraperpage.com/cities/?buildingID=85186)

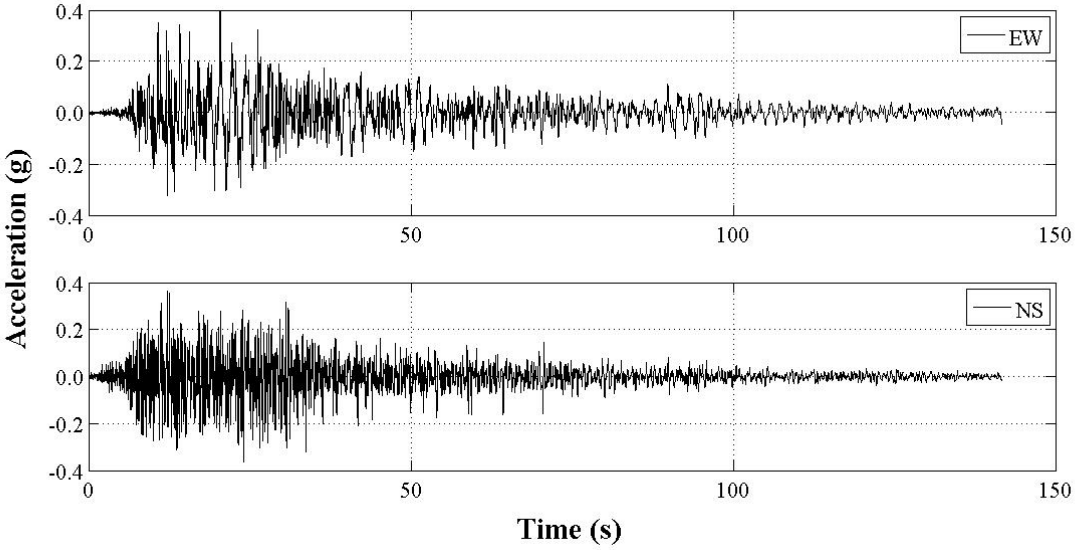

Fig. 2 - Ground motion from Colegio Inmaculada Concepción

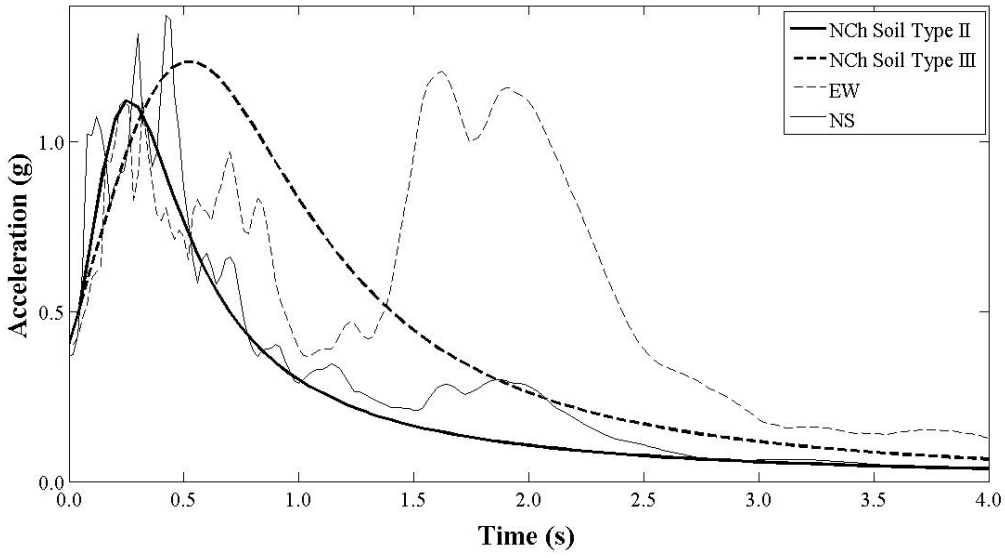

Fig. 3 - Design-level response spectra and 5%-damped response spectra from the ground motion record in Concepción

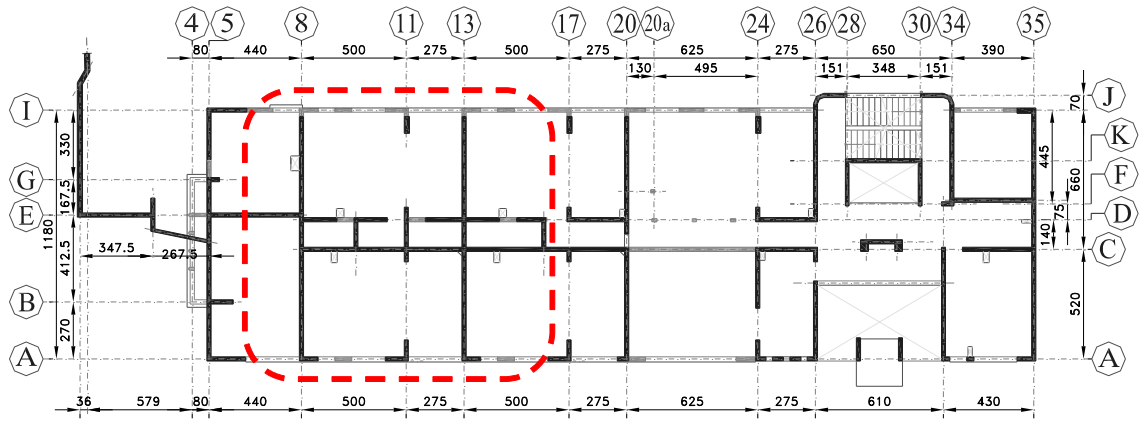

Fig. 4 - Alto Rio building first-floor plan. Dashed line encloses portion of building modeled in the nonlinear static analysis (Unit: cm) (Note: 1 cm = 0.3937 in)

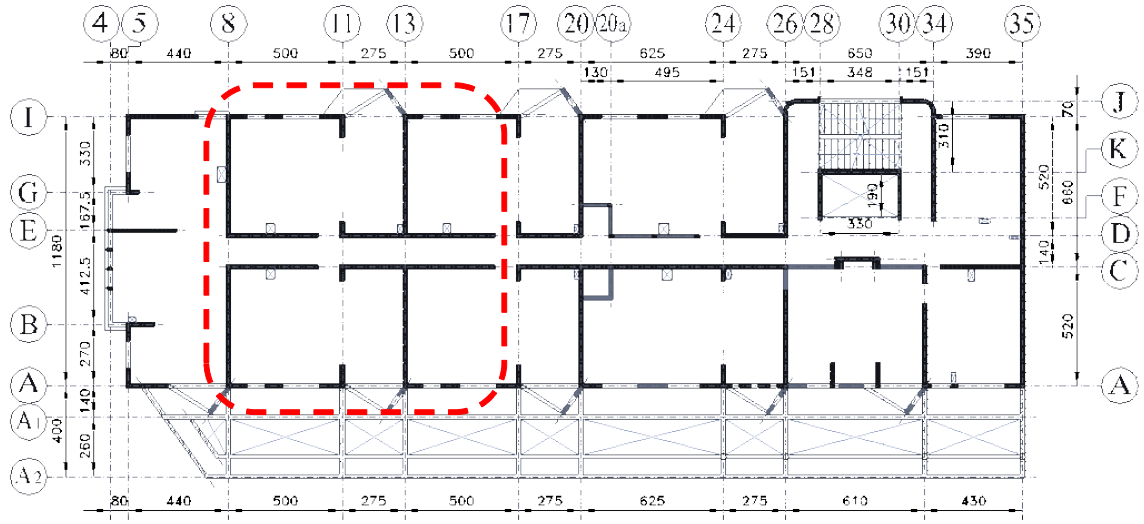

Fig. 5 - Alto Rio building second-floor plan. Dashed line encloses portion of building modeled in the nonlinear static analysis (Unit: cm) (Note: 1 cm = 0.3937 in)

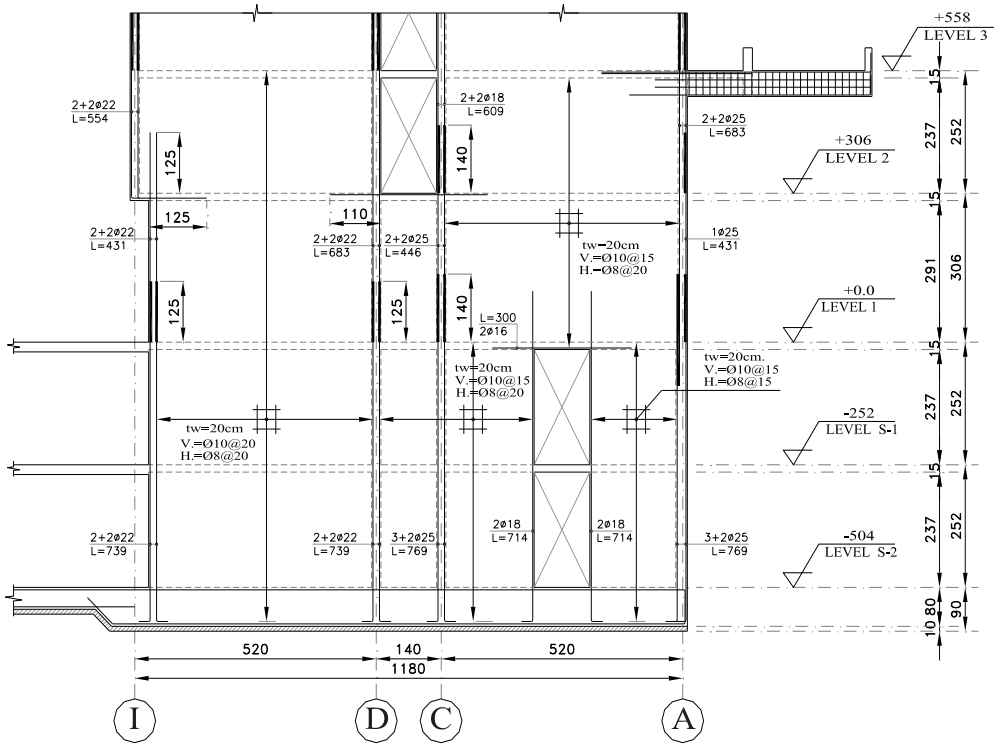

Fig. 6 - Alto Rio building axis 8 elevation view (Unit: cm) (Note: 1 cm = 0.3937 in)

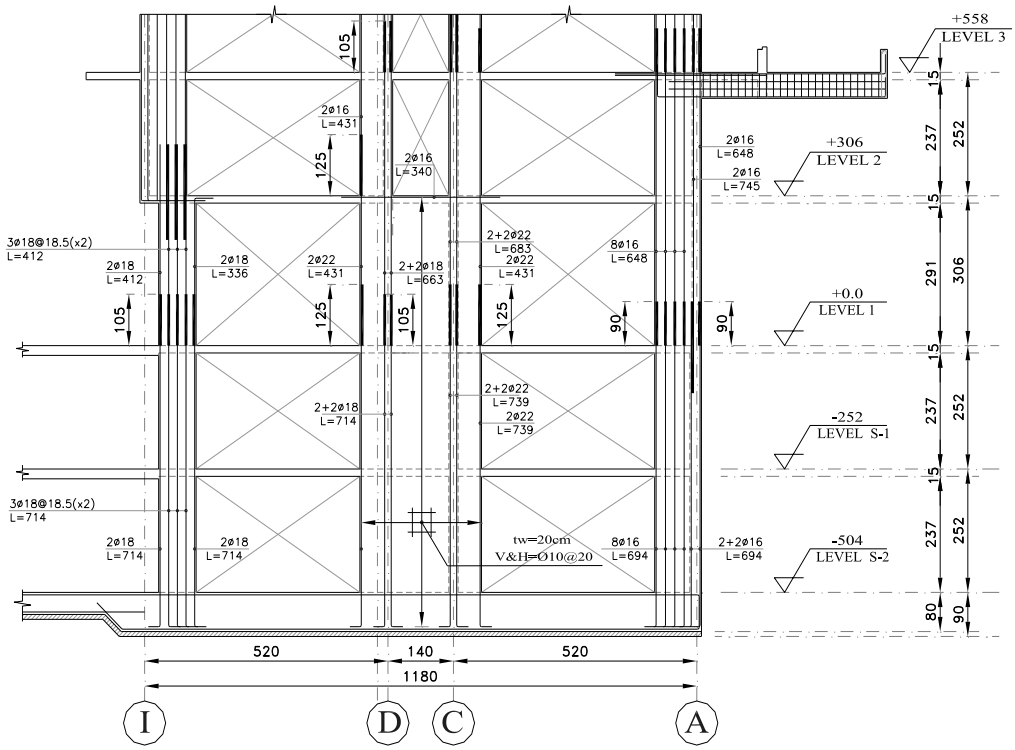

Fig. 7 - Alto Rio building axis 11 elevation view (Unit: cm) (Note: 1 cm = 0.3937 in)

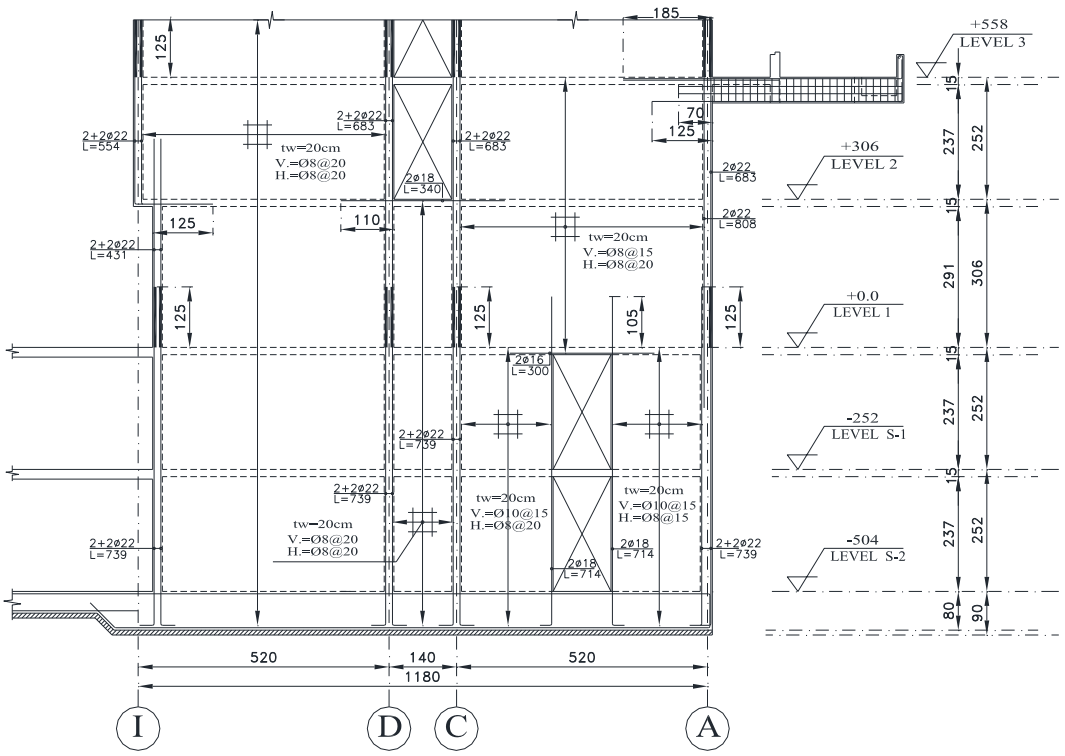

Fig. 8 - Alto Rio building axis 13 elevation view (Unit: cm) (Note: 1 cm = 0.3937 in)

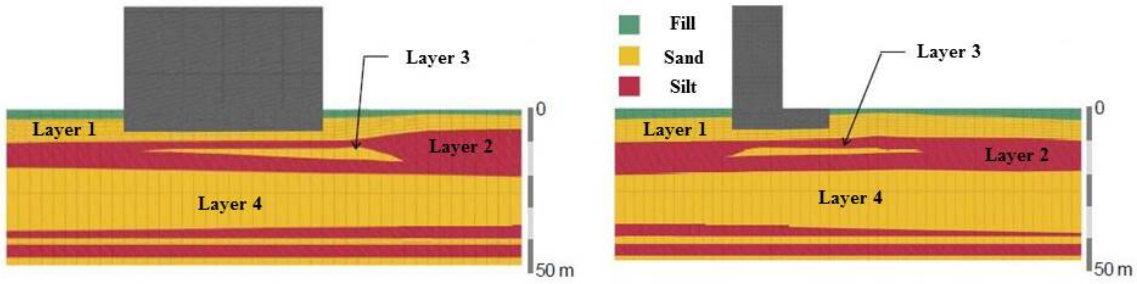

(a) View in transverse direction (b) View in longitudinal direction

Fig. 9 - Properties of Alto Rio building Site (after IDIEM, 2010) (Note: 1 m = 3.28 ft)

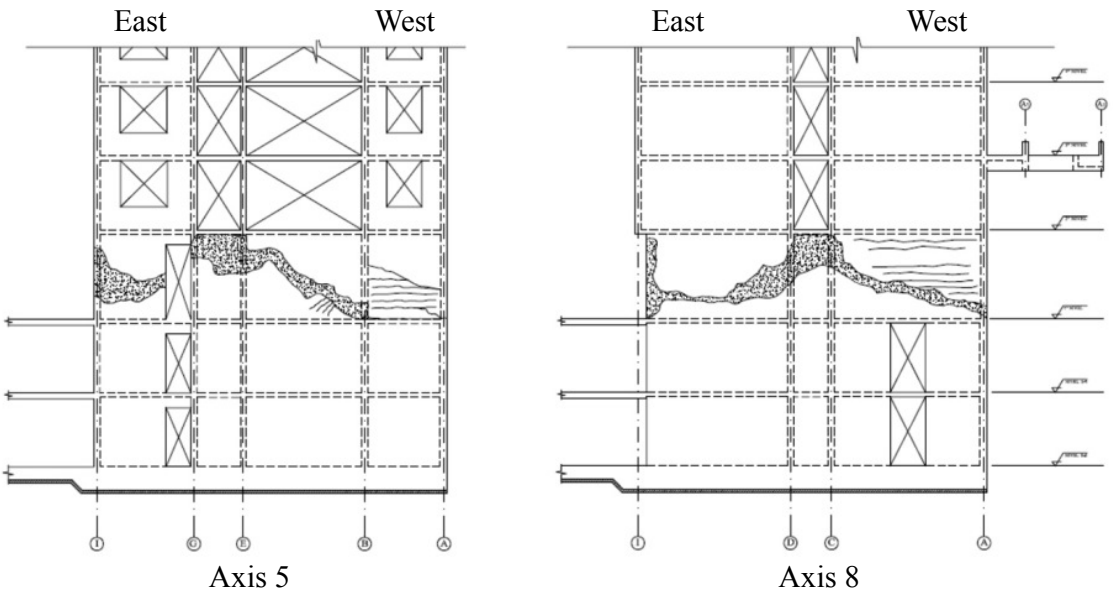

Fig. 10 - Sketch of damage on axes 5 and 8 (after IDIEM, 2010)

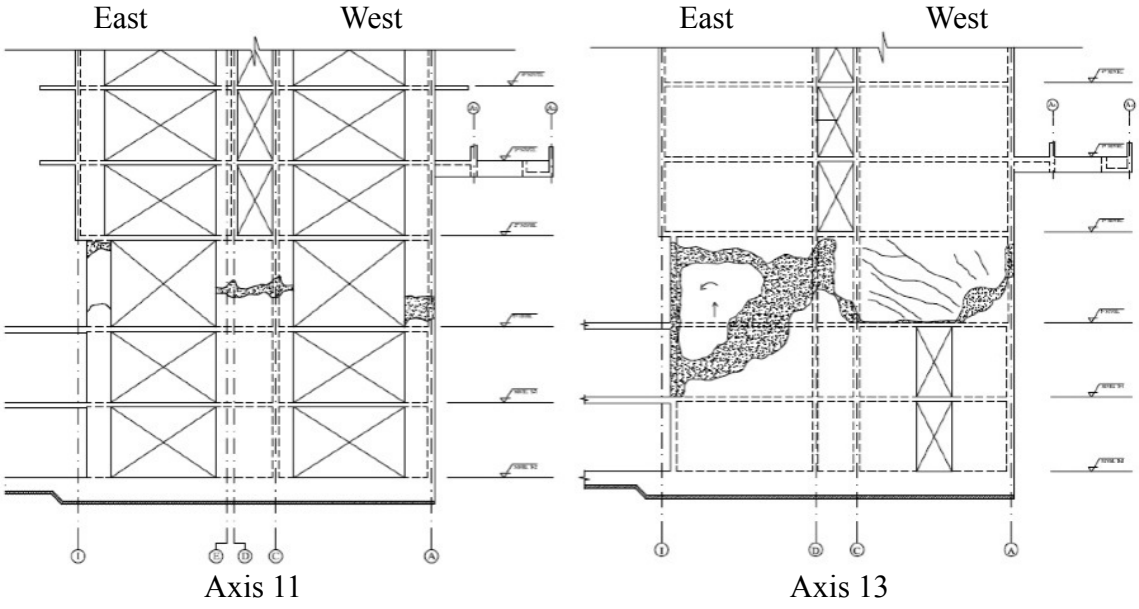

Fig. 11 - Sketch of damage on axes 11 and 13 (after IDIEM, 2010)

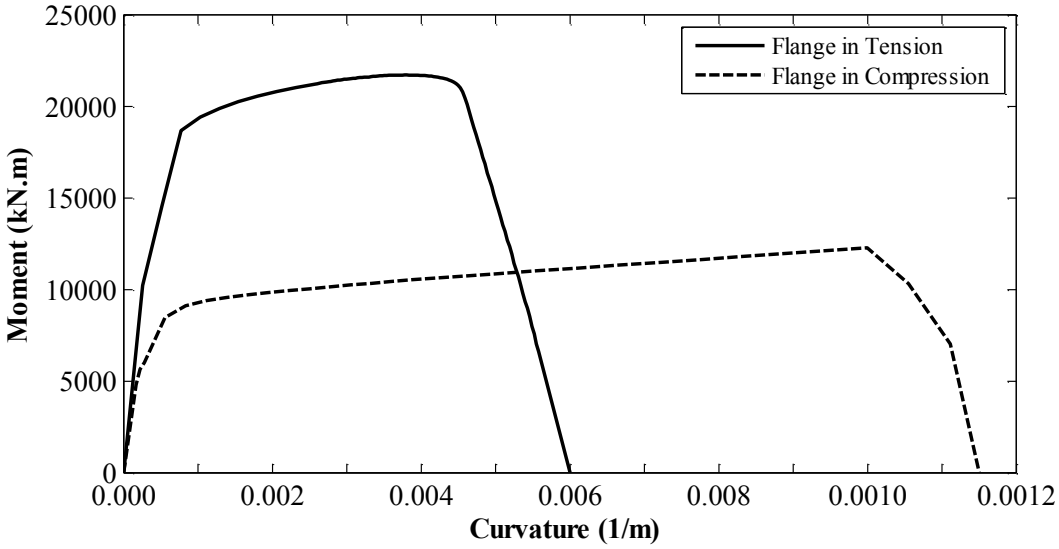

Fig. 12 - Moment Curvature analysis of the east wall on axis 13 (Note: 1 kN.m = 0.7375 kip.ft)

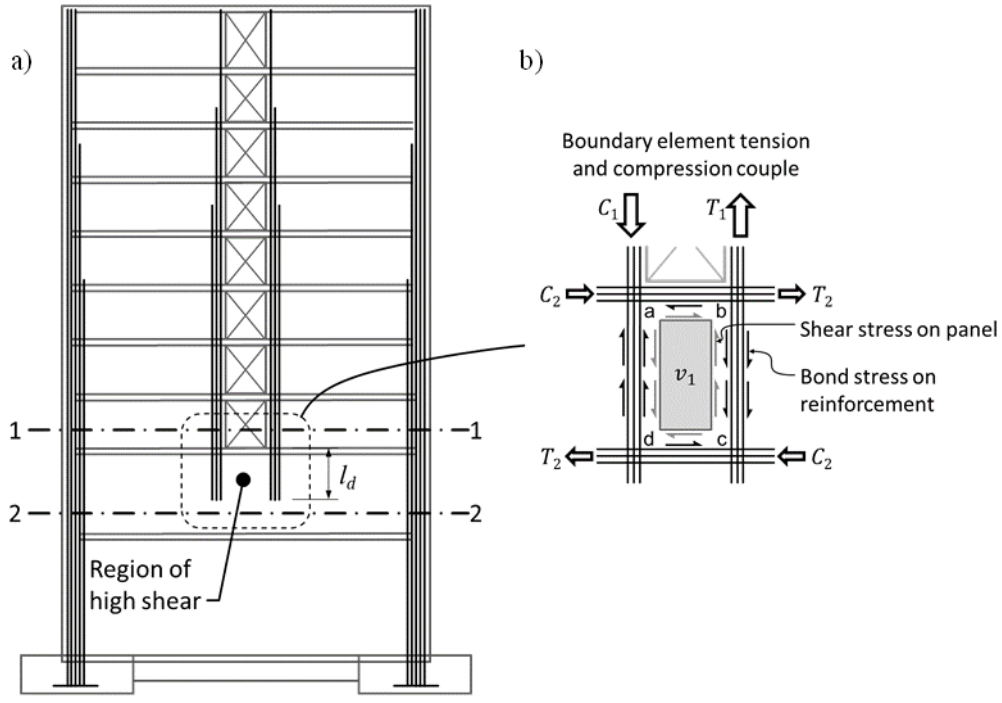

Fig. 13 - (a) Region of high shear stress in solid wall panel below the stack of openings (b) Solid wall panel shear and tension/compression chords

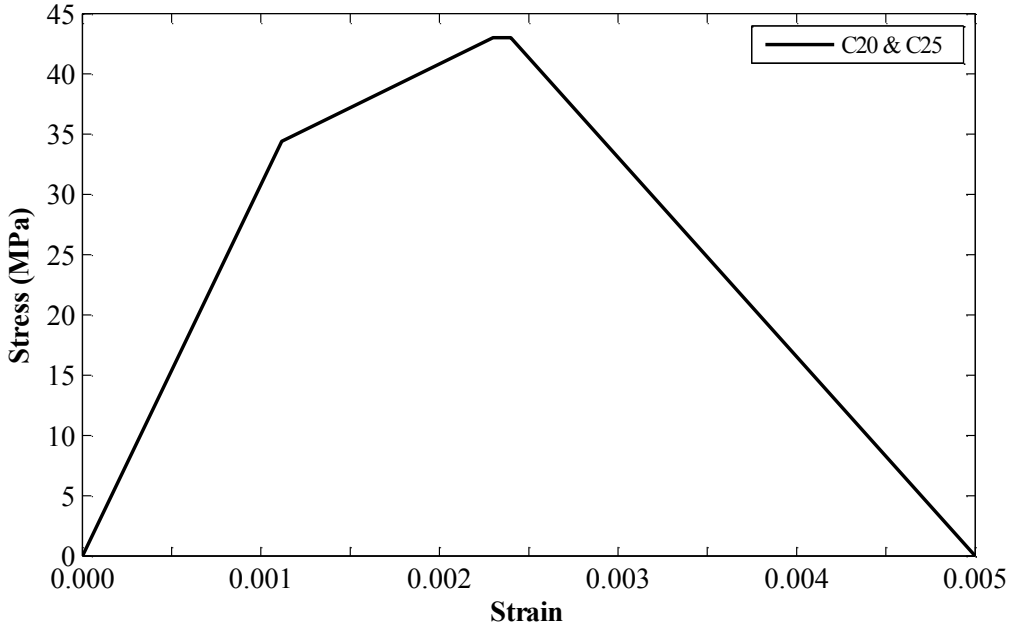

Fig. 14 - Concrete stress-strain relation (positive values are compressive) (Note: 1 MPa = 145 psi)

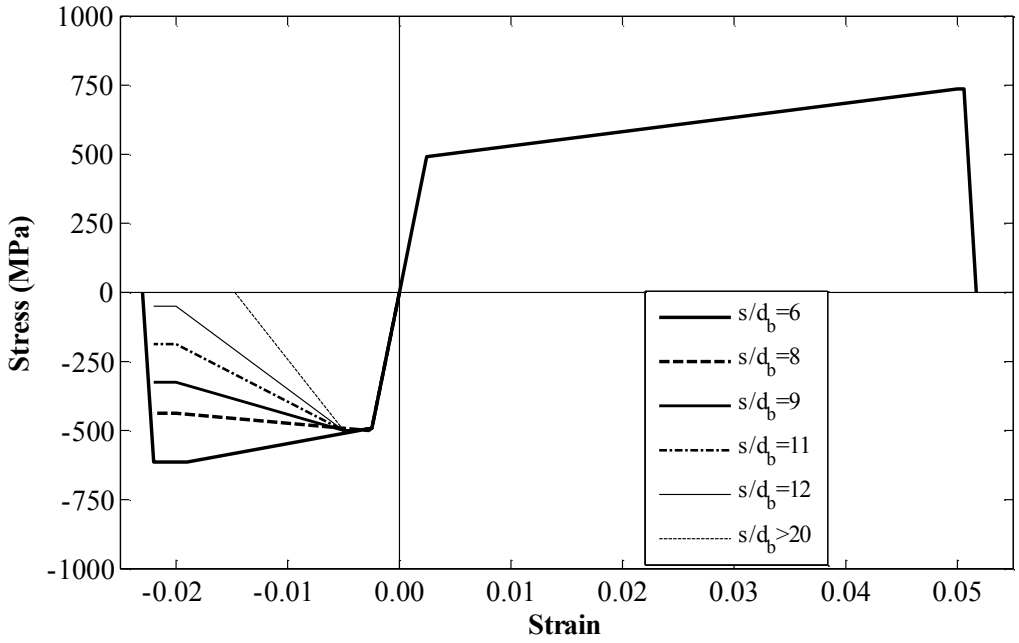

Fig. 15 - Reinforcing steel stress-strain relation (positive values are tensile) (Note: 1 MPa = 145 psi)

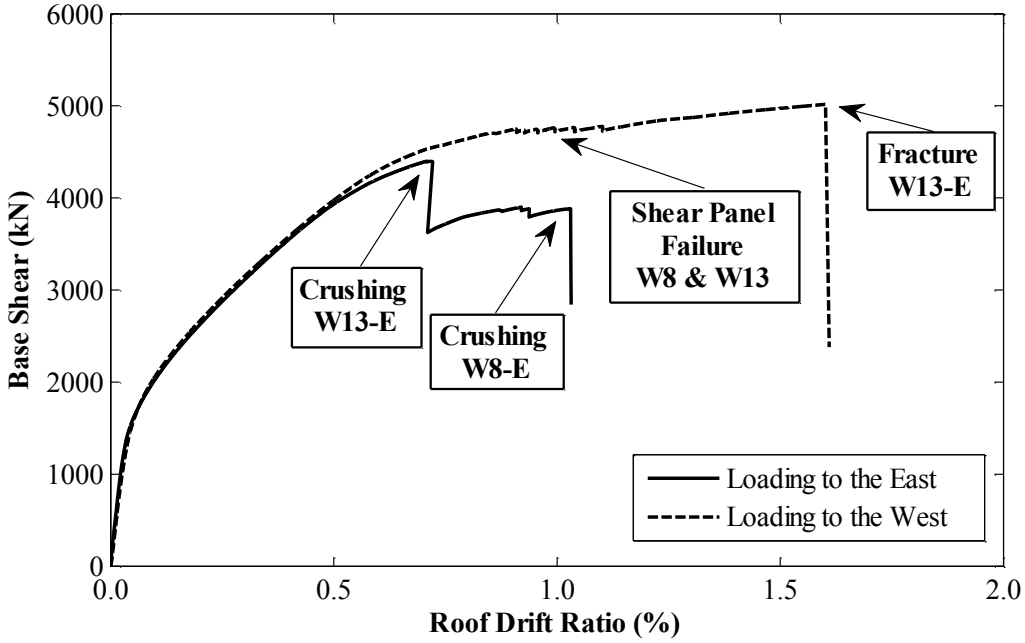

Fig. 16 - Base Shear – Drift relationship of nonlinear static analysis (Note: 1 kN = 0.2248 kips)

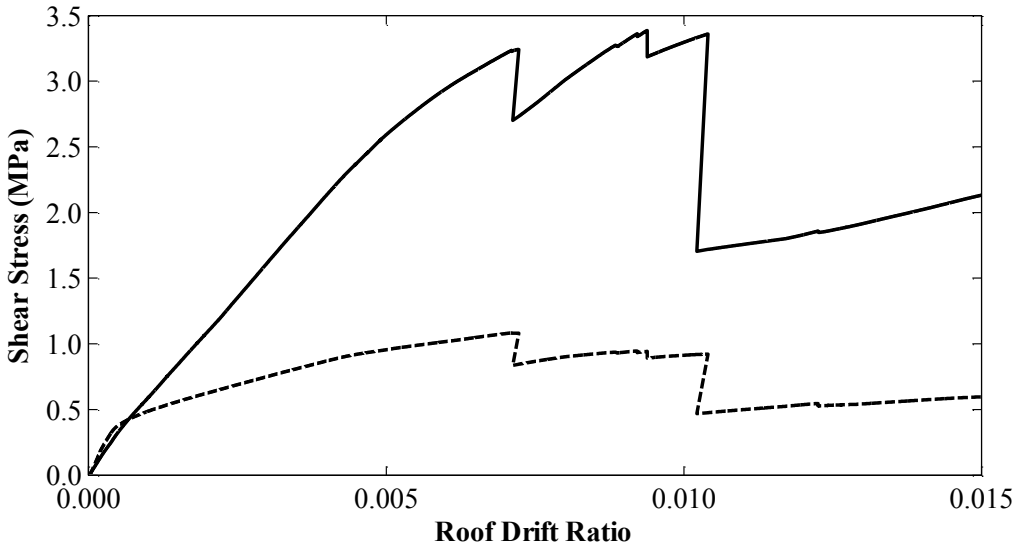

Fig. 17 - Shear stress – roof drift ratio relationship for solid wall panel below the stack of openings and for entire wall in story 1, using a linear model for the solid wall panel. Stress for the solid wall panel is the average value over the height of the story below the stack of openings. (Note: 1 MPa = 145 psi)

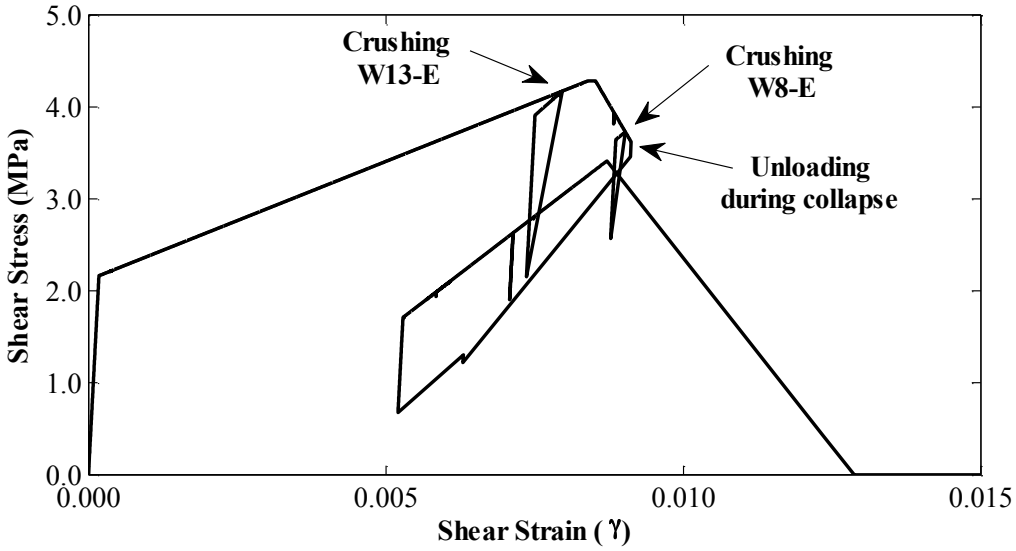

Fig. 18 - Shear stress – strain relationship of the solid wall panel below the stack of openings along axis 13 of the Alto Río building (Note: 1 MPa = 145 psi)

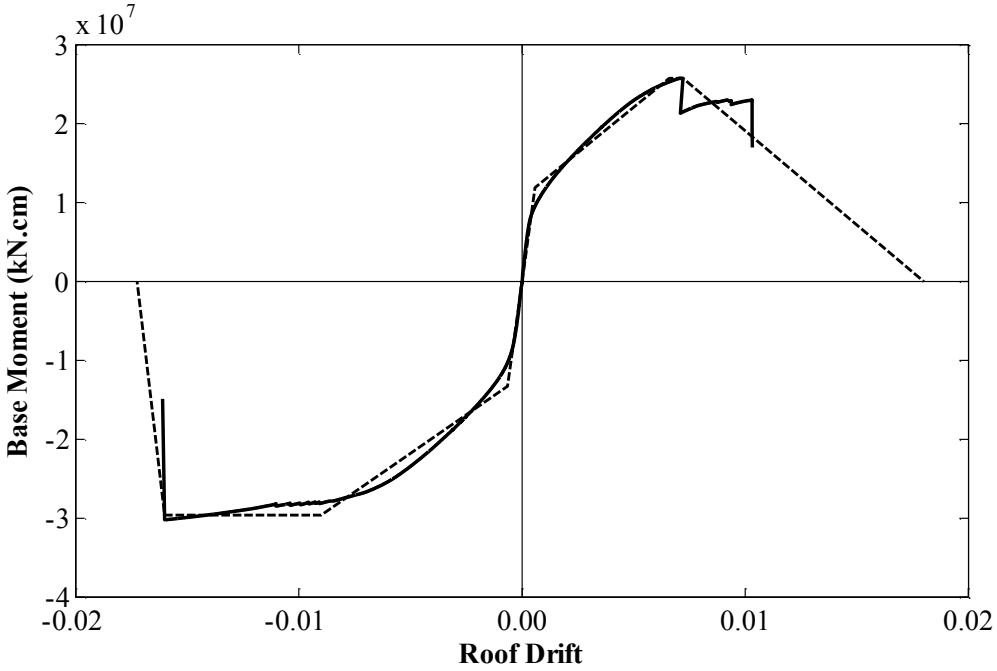

Fig. 19 - Comparison of moment-rotation relations for the SDOF model and the scaled nonlinear static analysis (Note: 1 kN.m = 0.7375 kip.ft)

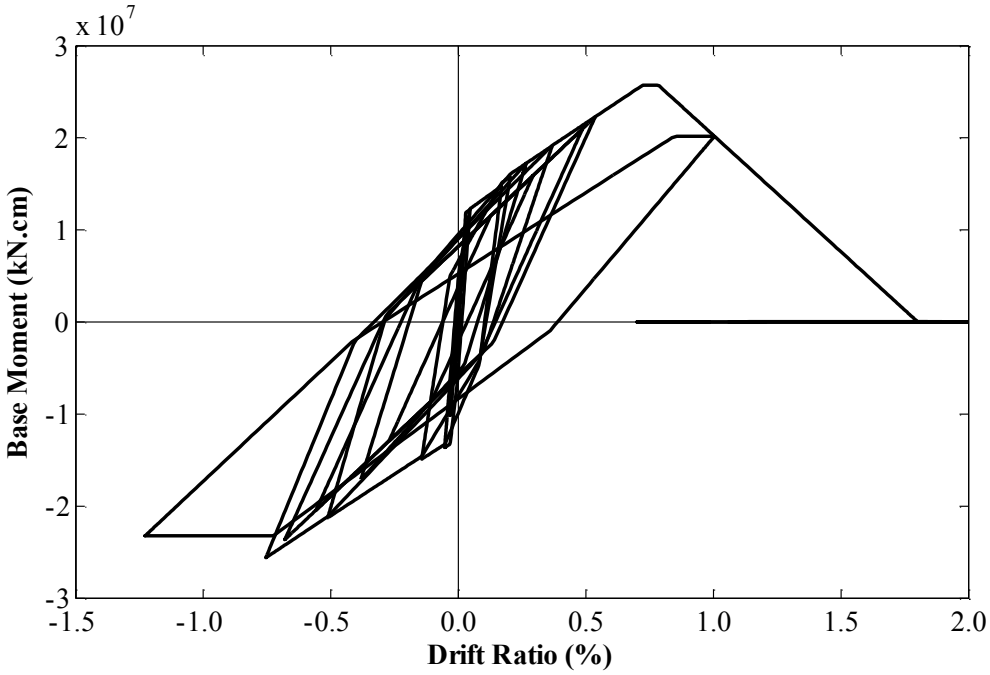

Fig. 20 - Moment–drift ratio response of the SDOF model under the Concepción ground motion (Note: 1 kN.m = 0.7375 kip.ft)

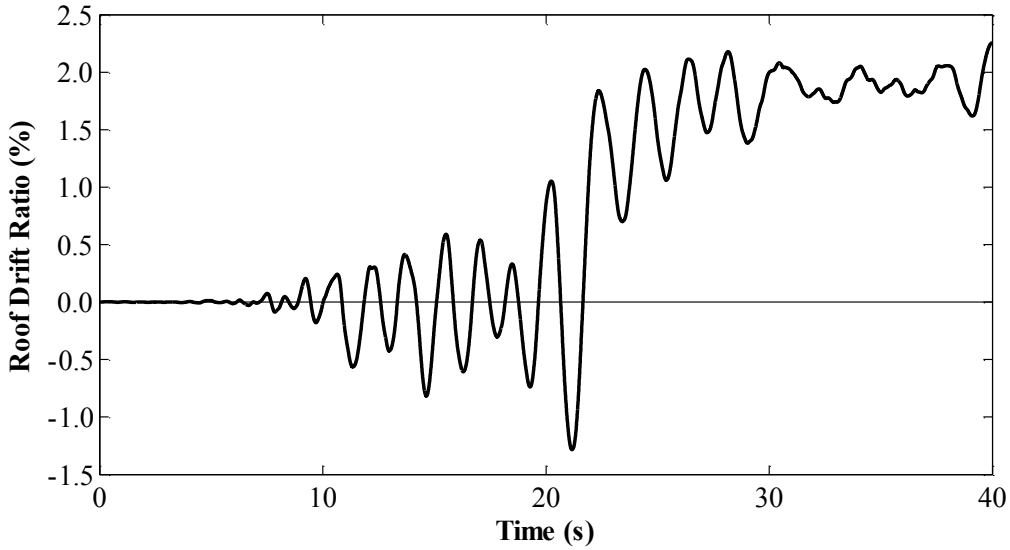

Fig. 21 - Roof drift ratio response history of the SDOF model subjected to the Concepción ground motion

(*) The number following the symbol ϕ refers to nominal diameter in mm.